AIAA JOURNAL
Vol. 33, No. 5, May 1995

Link Between Flow Separation and Transition Onset

J. A. Masad* and M. R. Malik†
High Technology Corporation, Hampton, Virginia 23666

The relationship between the location of boundary-layer separation and transition onset in compressible subsonic flow is studied. The flow separation considered in this study is caused by a localized adverse pressure gradient that results from a single roughness element (a hump) on an otherwise smooth flat plate. The mean flow is computed with the interacting boundary-layer (IBL) approach, and a quasiparallel stability analysis of the resulting profiles is performed. The N-factor criterion with $N = 9$ is used to correlate transition. The effects of unit Reynolds number, hump location, hump length, and freestream Mach number on the relationship between separation and transition location are evaluated. Our results support the customary assumption that the separation location can be taken as the transition onset location in a certain parameter space; however, this assumption is not valid in other ranges of the parameter space, particularly at low unit Reynolds numbers, for short humps, and at relatively high freestream Mach numbers.

I. Introduction

EXPERIMENTAL studies[1,2] and previous theoretical investigations[3–6] show that separation enhances significantly the instability of a boundary layer. Therefore, the onset location of laminar-turbulent transition is clearly linked with the location of boundary-layer separation. It was found[5,7] that as the height of a roughness element increases from zero (no roughness), the flow over the roughness element gets destabilized, and the disturbance growth rate increases. The disturbance growth rates were found to increase dramatically when the roughness height reached a critical value corresponding to incipient separation. When the roughness element height exceeds this critical value (that is, larger than the value causing separation) the predicted transition location using the empirical e^9 method was found by Masad and Nayfeh[7] and Masad and Iyer[5] to almost coincide with the location of separation. This result is in agreement with available experimental data (see, for example, Fage and Preston[8] and Dryden[9]). However, we are unaware of any theoretical investigation which focuses on quantifying the relationship between the separation and transition locations and the possible variation of this relationship in the large parameter space. In aircraft icing studies, for example, the transition location is normally assumed to be the same as the location of separation due to ice accretion. There are no theoretical studies which evaluate the accuracy of this assumption under different flow and icing conditions and for different surface configurations.

The separation considered in this study is due to the presence of a roughness element on a surface. For actual aerodynamic surfaces, roughness could result from manufacturing, degradation of the material (corrosion), rain erosion, insect impingement, and icing. Furthermore, the aerodynamic surfaces might include steps and gaps such as the steps at the joints between the wing and control surfaces on airplane flaps.

A few theoretical studies examine the effect of a single roughness element (that might induce flow separation) on stability and transition in compressible subsonic flow over a flat plate. A review of the effect of surface imperfections on the stability of laminar boundary layers is given by Nayfeh.[10] A detailed study that focuses on transition prediction and control in compressible subsonic flow over a hump is given by Masad and Iyer.[5] As we have already mentioned, earlier studies demonstrate that when flow separates, the disturbance growth rate increases considerably as would be expected. However, no detailed quantitative evaluation of the relationship between separation and transition onset locations was made in any of these studies. In this work, we perform a parametric study to quantify the relationship between the locations of transition onset and separation. Because of the large parameter space, we restrict our study to the separation caused by a single, two-dimensional roughness element (a hump) in compressible subsonic flow over a flat plate.

Received Jan. 28, 1994; revision received July 28, 1994; accepted for publication Aug. 18, 1994.

*Research Scientist. Senior Member AIAA.
†Chief Scientist. Associate Fellow AIAA.

II. Formulation and Methods of Solution

We consider compressible subsonic flow over a hump on a flat plate (Fig. 1). The hump shape is given by

$$y = \frac{y^*}{L^*} = \left(\frac{h^*}{L^*}\right) f(z) = h f(z) \tag{1}$$

where

$$z = 2\frac{(x^* - L^*)}{\lambda^*} = 2\frac{(x-1)}{\lambda} \tag{2}$$

and

$$f(z) = \begin{cases} 1 - 3z^2 + 2|z|^3 & \text{if } |z| \le 1 \\ 0 & \text{if } |z| > 1 \end{cases} \tag{3}$$

Here, h^* is the dimensional height, and λ^* is the dimensional length of the hump with the center located at $x^* = L^*$.

The boundary-layer mean flow over this hump is computed by solving the interacting boundary-layer (IBL) equations; the mean flow is easily computed within and outside the separation bubble. The flow over the hump can be analyzed using IBL theory,[11] triple-deck theory,[12,13] or by solving the Navier–Stokes equations. In the IBL[11] theory, the Prandtl transposition theorem is used with the Levy–Lees variables to obtain the nonsimilar boundary-layer equations and the corresponding boundary conditions. The upstream initial condition is taken to be that of a flow over a smooth flat plate. To account for the viscous-inviscid interaction, the inviscid flow over the displaced surface is calculated with the interaction law, which relates the edge velocity to the displacement thickness. Then, the thin-airfoil theory is used to supply the relation between the inviscid surface velocities with and without the boundary layer; it is also used to calculate the inviscid surface velocity in the absence of the boundary layer. The continuity equation is then manipulated and combined with the interaction law to yield a single equation that can be solved simultaneously with the nonsimilar boundary-layer equations and boundary conditions. The reliability of the IBL to produce mean-flow profiles that are accurate enough to be used in linear stability analysis was established by Ragab et al.[4]

In the IBL computations, the interaction region is taken to be in a conservative range that extends from a location close to the leading

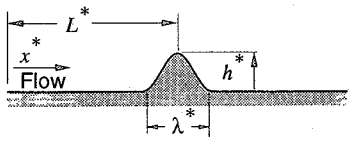

(Not to scale)

Fig. 1 Hump on flat plate.

edge to a location way downstream of the hump. The step size in the streamwise direction is uniform with $\Delta x = 0.005$. For a hump length λ of 0.2, this results in 40 points equally spaced over the hump length. In the transverse direction, a stretched grid is used with $\Delta\eta = 0.03$ and $\Delta\eta_j = 1.03\Delta\eta_{j-1}$ for $j = 2, \ldots, N$. The freestream boundary conditions are applied at $\eta_N = 15$. Computations were performed for different sets of flow and roughness parameters with smaller Δx, smaller $\Delta\eta_1$, and larger η_N, and the resulting profiles and their stability characteristics showed that the grid used in the computations ($\Delta x = 0.005$, $\Delta\eta_1 = 0.03$, and $\eta_N = 15$) results in grid-independent solutions.

The location of transition onset is predicted by performing a linear, quasiparallel spatial stability analysis of the mean-flow profiles and by using the empirical e^N method (with N equal to 9). Navier–Stokes computations by Gruber et al.[14] show that the error introduced by the quasiparallel assumption is not too severe. Van Dam and Elli[15] also performed Navier–Stokes computations and evaluated the effect of nonparallelism and nonlinearity. For the selected disturbance frequencies, they found noticeable difference between the Navier–Stokes solution and the Orr–Sommerfeld theory. However, we believe that the difference in the integrated growth (N factors) is small enough for the purposes of transition correlation in these flows. The agreement of the measured transition locations in the natural transition experiment of Fage[1] with the locations predicted[3,5] by the e^N method for flow over a roughness element demonstrates the reliability of this method in predicting the transition location for the flow under consideration. The linear stability calculations were performed using the IMSL subroutine B2PFD coupled with a Newton–Raphson iteration on the eigenvalue. The subroutine B2PFD is based on the code PASVA3 which was developed by Pereyra,[16] and it uses second-order accurate finite differences with deferred correction. In the freestream, asymptotic boundary conditions which utilize the boundedness of the disturbance in the freestream are used.

In the linear stability analysis of the mean flow over the hump, only two-dimensional disturbances are considered because, as pointed out by Mack,[17] disturbances in subsonic boundary layers (with a freestream Mach number M_∞ up to approximately 0.8) are most amplified when they are two dimensional. The frequency parameter F is defined as

$$F = \frac{2\pi\nu_\infty^*}{U_\infty^{*2}} f \tag{4}$$

where f is the dimensional frequency in hertz, ν_∞^* is the dimensional freestream kinematic viscosity, and U_∞^* is the dimensional freestream streamwise velocity. The frequency parameter F remains constant for the same physical wave as it propagates downstream. The freestream Reynolds number is denoted by Re and is defined as

$$Re = U_\infty^* L^*/\nu_\infty^* \tag{5}$$

where L^* (Fig. 1) is the dimensional distance from the leading edge of the plate to the center of the hump. The local Reynolds number Re_x is given by

$$Re_x = U_\infty^* x^*/\nu_\infty^* \tag{6}$$

and x^* (Fig. 1) is the dimensional distance measured from the leading edge of the plate. The predicted transition location is taken to be the point where the N factor of the disturbance reaches a value of 9 in the shortest distance measured from the leading edge. The value of Re_x at that location is denoted by $(Re_x)_{N=9}$.

III. Results

Figure 2 shows the streamwise variation of the pressure coefficient C_p for the incompressible flow over the hump shown in Fig. 1 and for a hump height h of 0.003 (which causes the flow to separate). Four regions of pressure gradient can be distinguished as we proceed downstream in the neighborhood of the hump: adverse, favorable, and a strong adverse followed by a mild favorable region. Away from the hump on either side, we recover the zero pressure gradient of a smooth flat plate.

It is well known that adverse pressure gradient destabilizes the flow whereas the favorable pressure gradient stabilizes it. The overall effect of the hump on the disturbance growth is destabilizing. However, several parameters can influence the relationship between the predicted transition location and the location of separation due to the hump. These parameters include the hump height, length, and location; the freestream unit Reynolds number; and the freestream Mach number. In this section, we present results that demonstrate these effects.

A. Flow Separation

Separation occurs when the adverse pressure gradient is sufficiently strong. The momentum of the gas as it moves against the adverse pressure gradient becomes too weak to overcome the viscous force; beyond a certain level of adverse pressure gradient, the flow is brought to rest, and backflow (separation) occurs. In this work, we consider the flow separation that results from a local adverse pressure gradient generated by a two-dimensional roughness element.

Previous computations[3,5] have shown that when separation occurs it begins at some point between the center and the end of the hump. We denote the Reynolds numbers based on the distance from the leading edge of the plate to the center and to the end of the hump by Re_C and Re_E, respectively. Because Re is based on the distance from the leading edge of the plate to the center of the hump, then

$$Re_C = Re \tag{7}$$

Furthermore, Fig. 1 shows that

$$Re_E = U_\infty^*\left(L^* + \frac{\lambda^*}{2}\right)\Big/\nu_\infty^*$$

Thus,

$$Re_E = \left(1 + \frac{\lambda}{2}\right)Re \tag{8}$$

where $\lambda = \lambda^*/L^*$ has been used. For example, when $\lambda = 0.2$, Eq. (8) gives $Re_E = 1.1Re$. Therefore, the traces of Re_C and Re_E in Fig. 3 correspond to

$$Re_x = Re_C = Re$$

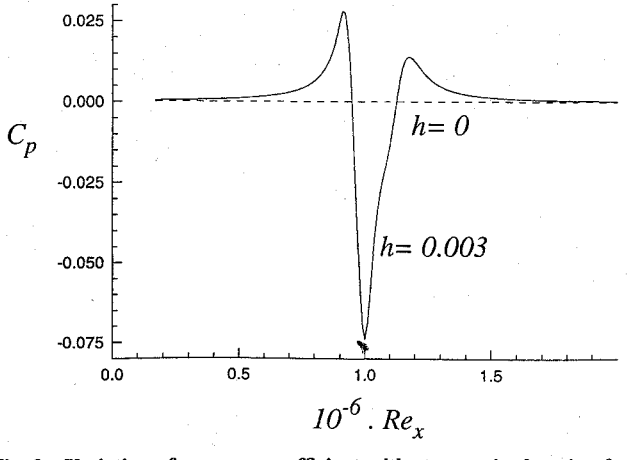

Fig. 2 Variation of pressure coefficient with streamwise location for separating incompressible flow with and without hump at $\lambda = 0.2$, $h = 0.003$, and $Re = 10^6$.

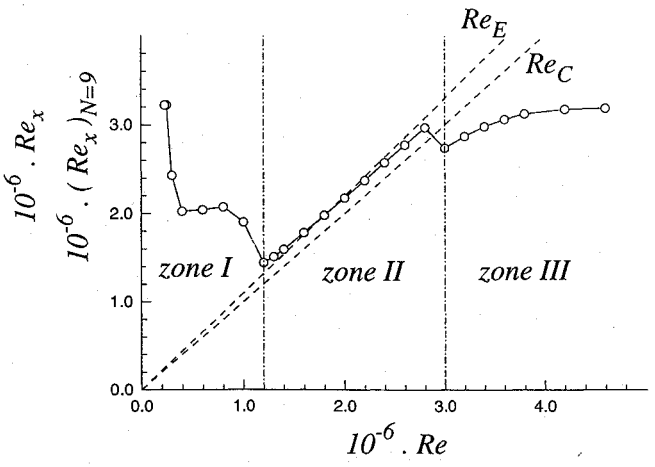

Fig. 3 Variation of local Reynolds numbers Re_C and Re_E and predicted transition Reynolds number with freestream Reynolds number for $M_\infty = 0$, $\lambda = 0.2$, and fixed hump location.

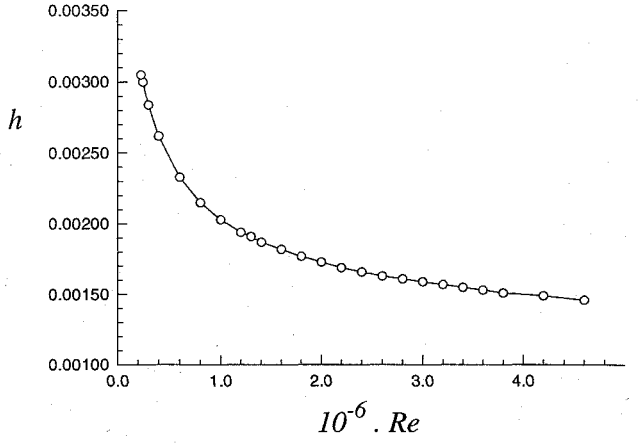

Fig. 4 Variation of hump height causing incipient separation with freestream Reynolds number for $M_\infty = 0$, $\lambda = 0.2$, and fixed hump location.

and

$$Re_x = Re_E = 1.1Re$$

respectively. These traces are shown by the dashed lines in the figure. Because the onset of separation is between the center and the end of the hump, it occurs at a value of Re_x between the two dashed lines.

B. Effect of Unit Reynolds Number

To study the effect of unit Reynolds number on the relationship between the locations of transition and separation, we considered a hump with a fixed length λ^* and a center at a fixed location L^*. Because $\lambda = \lambda^*/L^*$, λ also remained fixed. We first considered an incompressible flow with $M_\infty = 0$ and $\lambda = 0.2$. The freestream Reynolds number Re given by Eq. (5) was varied by varying the unit Reynolds number. For each value of Re, the hump height h that caused incipient separation was determined. Then, the predicted transition location in the flow over a hump with that particular height was computed. As the unit Reynolds number decreased, the hump height that caused incipient separation increased (Fig. 4). This result agrees with both the theoretical results of Masad and Iyer[5] and the experimental results of Holmes et al.,[2] who noted that an increase in the altitude (which decreases the unit Reynolds number) reduces the length of the separation bubble caused by a step. The result also agrees with the wind-tunnel experimental observation of Fage and Preston[8] who noticed that initially the flow over a wire mounted around a body of revolution was smooth without forming a wake and as the velocity of the flow was increased (which increases the unit Reynolds number) a wake was formed behind the wire.

The predicted transition Reynolds number variation with the freestream Reynolds number is shown in Fig. 3. The predicted transition Reynolds numbers presented throughout this work were computed by searching for the most amplified frequency [the frequency that results in the lowest $(Re_x)_{N=9}$ for a given set of conditions]. In this search, F was varied in steps of 10^{-6}. To determine the hump height responsible for incipient separation, h was varied in steps of 10^{-5}.

Note in Fig. 3 that at each value of Re a reduction in the hump height from the value that causes incipient separation results in no separation; thus, there is an increase in the predicted transition Reynolds number. Therefore, at each Re, a reduction in the hump height below the incipient separation value corresponds to transition Reynolds numbers above the solid line, and an increase in the height above the incipient separation value corresponds to transition Reynolds numbers below the solid line. The assumption that transition will occur at the onset of separation implies that it will occur at values of Re_x within the two dashed lines in Fig. 3. Figure 3 readily shows that although this assumption is reasonable at moderate values of Re (zone II) it is not valid at low (zone I) and high (zone III) values of Re.

In zone I of Fig. 3, the transition location is far downstream of the separation point, and the assumption that the transition onset location is the separation location is a conservative assumption. In the wind-tunnel experimental study of Fage and Preston[8] for flow past a wire mounted on a body of revolution it was noticed that at a certain freestream velocity the flow formed separation vortices but the flow was laminar far downstream of the wire. Increasing the freestream velocity moved the transition point closer to the wire. This observation is in agreement with the predictions shown in zone I of Fig. 3. The behavior at low values of Re in zone I can be explained by the following argument. Low values of Re correspond to locations far upstream of the first neutral point of flow over a smooth flat plate. In that region, the disturbances are strongly damped. Although the flow separates, it accumulates an amplification factor that fails to reach a value of 9. Then the flow encounters a smooth flat-plate region that is still ahead of branch I; therefore, the previously accumulated growth is canceled by the decay prior to reaching branch I. Hence, in this region, the predicted transition Reynolds number is again that of a flow over a smooth flat plate. This argument explains the variation of $(Re_x)_{N=9}$ with Re at low values of Re in zone I of Fig. 3. The behavior in the rest of zone I is more complicated and is dictated by the relative locations of the adverse and favorable pressure gradient regions with respect to the smooth flat-plate lower neutral point. The situation in this region of zone I is similar to placing a vibrating ribbon (in an experiment) close to the leading edge and exciting it with a relatively large amplitude. In this case, the disturbance will reach the first neutral point with a vanishingly small amplitude due to the strongly stable region between the leading edge and the first neutral point. We point out that although placing a roughness element anywhere on the plate enhances the receptivity, placing the roughness element close to the leading edge along with its associated pressure gradient is expected to cause further enhancement of receptivity due to the pressure gradient at the leading edge (see Goldstein and Hultgren[18]).

Zone I of Fig. 3 clearly shows the importance of computing the mean flow beyond the separation point in zone I. Although the boundary-layer equations are capable of predicting the separation location, they fail to march through it; to compute the mean flow beyond separation, one must use a Navier–Stokes (NS) solver, of a viscous-inviscid interaction theory such as the IBL[11] equations used in this study, or triple-deck theory.[12,13] The IBL procedure requires computer time of one to two orders of magnitude less than is required by the NS solver, to the same level of accuracy.

A large value of Re corresponds to a location that is far downstream of the second neutral point for Tollmien–Schlichting instability in the boundary layer over a smooth flat plate. In this case, the N factor reaches a value of 9 before it even gets to the hump. Therefore, large values of Re generate a value of $(Re_x)_{N=9}$ that is the same as that of a smooth flat plate, namely, $(Re_x)_{N=9} \approx 3.2 \times 10^6$. This is shown clearly in zone III of Fig. 3 where the predicted transition Reynolds number at large values of Re saturates to a constant value

of approximately $(Re_x)_{N=9} \approx 3.2 \times 10^6$. As Re decreases from the considered large value, the hump location is downstream but moves closer to the second neutral point of flow over a smooth flat plate. At a certain value of Re, the flow begins to feel the mild adverse pressure gradient at the beginning of the hump. Because the adverse pressure gradient is destabilizing, the transition location moves upstream. A further decrease in Re increases the effect of the adverse pressure gradiant, which decreases $(Re_x)_{N=9}$ to a point where the flow stability has been fully affected by the first adverse pressure gradient region, and this corresponds to the lowest value of $(Re_x)_{N=9}$ in zone III of Fig. 3. At values of Re lower than this point, the flow begins to be influenced by a favorable pressure gradient region, and because the favorable pressure gradient is stabilizing, $(Re_x)_{N=9}$ increases the maximum value of $(Re_x)_{N=9}$ in zone II of Fig. 3. Then a further decrease in Re causes the flow to begin to be influenced by the second much stronger adverse pressure gradient region which also causes flow separation. In this region, $(Re_x)_{N=9}$ begins to decrease as shown in zone II.

Although, these results are obtained for the specific case of flow over a roughness element, the conclusions drawn are believed to be applicable to boundary-layer transition over natural laminar flow airfoils where flow separation occurs beyond the location of pressure minimum. Thus, if unit Reynolds number is sufficiently low, transition will occur past the separation point; and if the unit Reynolds number is high, transition will occur ahead of the separation point. These two cases correspond to zones I and III of Fig. 4, respectively. At some intermediate values of unit Reynolds number, transition location will coincide with the separation location.

C. Effect of Roughness Location

To study the effect of the hump location on the relationship between separation and transition onset locations, Re is varied by varying L^*, which is the dimensional distance from the leading edge to the center of the hump. To keep the dimensional hump's length λ^* fixed, $\lambda = \lambda^*/L^*$ must vary in accordance with the variation of L^*. Therefore, we choose the reference quantities.

$$Re_0 = U_\infty^* L_0^*/\nu_\infty^*$$

$$\lambda_0 = \lambda_0^*/L_0^*$$

therefore,

$$Re = Re_0 L^*/L_0^* \tag{9}$$

$$\lambda = \lambda_0 L_0^*/L^* \tag{10}$$

Note that as Re decreases, λ increases; therefore, the nondimensional height h required to induce separation increases. For the results presented in this section, Re_0 is taken as 2×10^6, and $\lambda_0 = 0.2$. Variation of the predicted transition Reynolds number with Re at $M_\infty = 0$ is shown in Fig. 5. The figure clearly shows that the approximation of the transition location by the separation location is reasonable, except at hump locations downstream of branch II of the neutral stability curve for a smooth flat plate. At hump locations close to the leading edge, the nondimensional hump height needed to cause separation increases significantly. At such locations of the roughness, even a relatively large height roughness element results in a somewhat significant transition Reynolds number. This result was clearly shown by Masad and Iyer,[5] and it is consistent with the flight test results of Braslow and Maddalon[19] for roughness on a swept wing and previous data of Von Doenhoff and Braslow[20] and Braslow et al.[21] for roughness on unswept wings. The result is also in agreement with wind-tunnel experimental observations of Fage and Preston[8] for flow past a wire mounted on a body of revolution.

At hump locations downstream of branch II of the neutral stability curve of a smooth flat plate, the N factor reaches a value of 9 before it gets to the hump; therefore, the transition Reynolds number is equal to that of flow over a smooth flat plate. The dashed lines in Fig. 5 indicate the locations (Reynolds numbers) of the center and the end of the hump. The contours of these lines are given by

$$Re_x = Re_C = Re$$

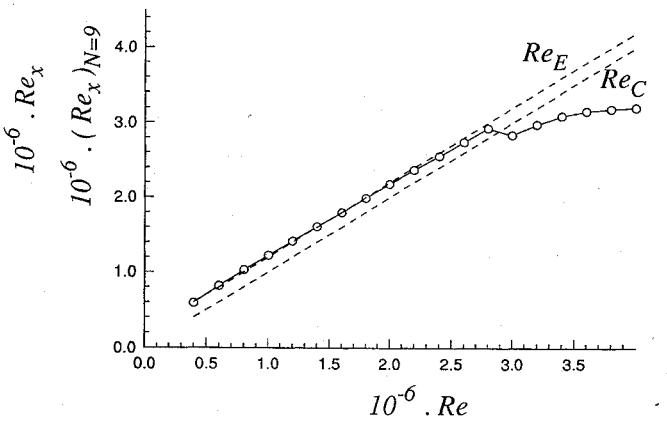

Fig. 5 Variation of Re_C, Re_E, and predicted transition Reynolds number with freestream Reynolds number for $M_\infty = 0$, $\lambda = 0.2$, $Re_0 = 2 \times 10^6$, and fixed unit Reynolds number.

From Eqs. (8–10), we obtain

$$\begin{aligned} Re_x = Re_E &= \left(1 + \frac{1}{2}\lambda_0 \frac{L_0^*}{L^*}\right) Re \\ &= Re + \frac{1}{2}\lambda_0 \frac{L_0^*}{L^*} Re_0 \frac{L^*}{L_0^*} \\ &= Re + \frac{1}{2}\lambda_0 Re_0 \\ &= Re + 0.2 \times 10^6 \end{aligned}$$

Therefore, Re_E is represented by an upward shift of Re_C, and the dashed lines in Fig. 5 are parallel.

D. Effect of Mach Number

An increase in the freestream Mach number M_∞ increases the value of the adverse pressure gradient in the flow over the hump, and this enhances separation.[22] Therefore, at the same freestream Reynolds number and hump length, the hump height that causes separation is expected to decrease as the freestream Mach number increases. When the flow separates, increasing the freestream Mach number increases the length of the separation bubble by shifting the separation location slightly upstream and shifting the reattachment location considerably downstream (see Masad and Nayfeh[22]). Such an increase in the size of the separation bubble due to compressibility was noticed experimentally by Larson and Keating.[23] Because the enhancement of separation has a destabilizing effect, the growth rates of disturbances in the adverse pressure gradient regions may increase as M_∞ increases. However, an increase in M_∞ in the zero pressure gradient regions away from the hump has a stabilizing effect. Reference 5 shows that the stabilizing effect of an increased M_∞ in the zero pressure gradient regions away from the hump overcomes the destabilizing effect in the adverse pressure gradient regions. Therefore, an increase in the freestream Mach number in flow over a hump shifts the predicted transition location downstream. This result is consistent with the need of larger diameter wires to trip the boundary layer as the Mach number increases (see, for example, Coles[24]).

To study the effect of the freestream Mach number on the relationship between the locations of transition and separation, we performed calculations similar to those carried out to produce the results in Fig. 3, but at $M_\infty = 0.8$. The freestream temperature was fixed at 300 K and the Prandtl number was 0.72. The results of these calculations are compared with the results at $M_\infty = 0$ in Fig. 6. The hump height needed to cause incipient separation decreases as M_∞ increases from 0 to 0.8. Furthermore, the results in Fig. 6 clearly demonstrate the stabilizing effect of an increased M_∞. The curve in Fig. 6 for $M_\infty = 0.8$ has the same features as that for $M_\infty = 0$, expect that it is shifted above and to the right.

Results similar to those in Fig. 5 at $M_\infty = 0$ were obtained for $M_\infty = 0.8$. Both sets of results as shown in Fig. 7. Figure 7 clearly

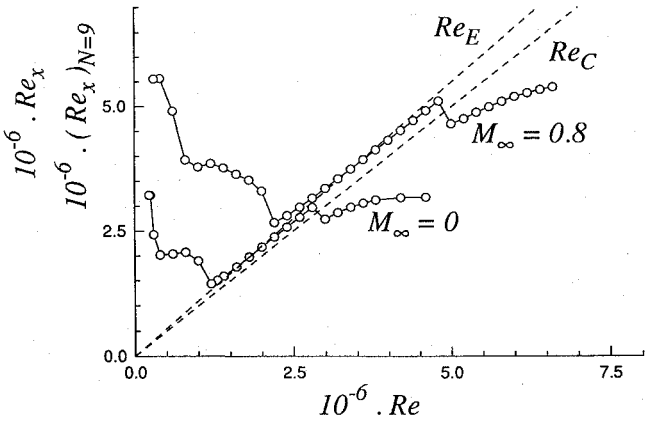

Fig. 6 Variation of Re_C, Re_E, and predicted transition Reynolds number with freestream Reynolds number for $\lambda = 0.2$ and fixed location of hump.

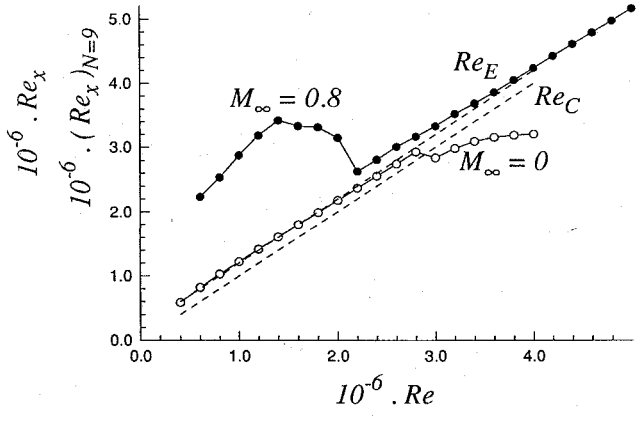

Fig. 7 Variation of Re_C, Re_E, and predicted transition Reynolds number with freestream Reynolds number for $\lambda = 0.2$ and fixed unit Reynolds number.

shows that an increase in M_∞ from 0 to 0.8 creates a region where the separation and transition locations are far apart. The reference quantities λ_0 and Re_0 for the results in Fig. 7 are the same as those for Fig. 5 ($\lambda_0 = 0.2$ and $Re_0 = 2 \times 10^6$).

E. Effect of Roughness Length

The effect of the length of a roughness element on flow instability and transition location is usually overlooked. Although the experimental correlations of Fage[1] and Carmichael[25] account for the effect of roughness length on transition location, the commonly used Re_k empirical correlation does not. The Re_k (see Morkovin[26]) is given by

$$Re_k = kU_k/\nu \tag{11}$$

where k is the roughness height, U_k the mean flow velocity at the height k in absence of the roughness, and ν is the kinematic viscosity. In the Re_k criterion, it is assumed that the flow is transitional on the roughness element itself when Re_k exceeds a certain critical value. In aircraft icing studies (see, for example, Hansman[27]) the critical value of Re_k is taken to be 600. Fage and Preston[8] indicated that the value is above 400 for the case of flow over a circular wire mounted on a body of revolution. It is clear from Eq. (11) that except for a circular wire the length of the roughness is not represented in Re_k. It was found by Masad and Iyer[5] that the length of a roughness element has a strong influence on inducing separation and triggering transition. For the same hump height and flow conditions, short humps induce separation and increase the size of the separation bubble. Furthermore, short humps enhance instability and move the transition location upstream. When the hump's length is smaller than a certain critical value (close to the value causing separation), the upstream movement of transition location was found to slow down considerably and the transition location saturates.

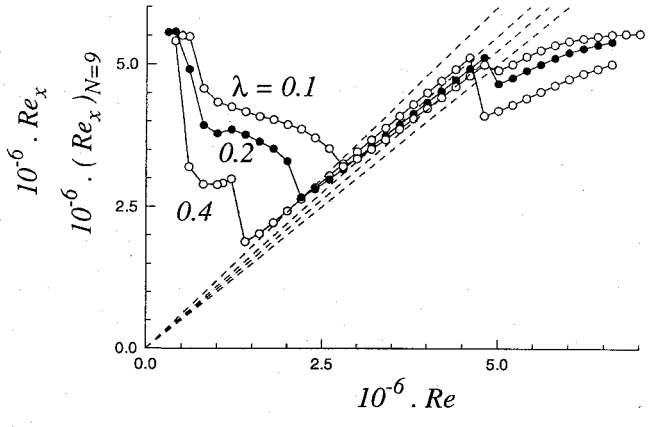

Fig. 8 Variation of Re_C, Re_E, and predicted transition Reynolds number with freestream Reynolds number for $M_\infty = 0$ and fixed location of hump.

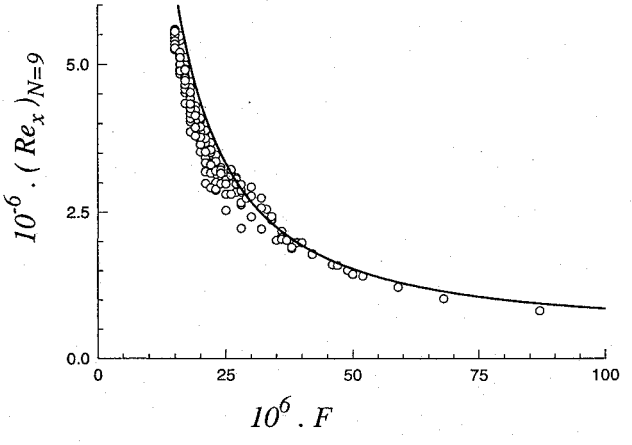

Fig. 9 Variation of transition Reynolds number with most amplified frequency: —, correlation and ○, direct calculations with incipient separation.

To study the effect of hump length on the relationship between the locations of separation and transition, we selected three hump lengths: $\lambda = 0.1, 0.2$, and 0.4. Calculations were performed at $M_\infty = 0.8$. The variation of the predicted transition location with Re (which was varied by changing the unit Reynolds number) at incipient separation was computed for all three hump lengths. The results are shown in Fig. 8. Figure 8 clearly shows that a reduction in the length of the hump causes zone I to shift considerably toward higher values of Re and causes only a slight shift in zone III.

F. Relationship Between Transition Reynolds Number and the Most Amplified Frequency

In all our performed calculations, the upstream movement of the transition location was accompanied by an increase in the disturbance frequency that caused transition. This finding agrees with the results in Ref. 5 for flow over a hump. It also agrees with the results of the analytical correlation of Masad and Malik[28,29] for subsonic flow over a smooth flat plate with different velocity and thermal boundary conditions. The analytical correlation[28,29] of the most amplified frequency with the transition Reynolds number is given by

$$(Re_x)_{N=9} = 254\Gamma \tag{12}$$

where

$$\Gamma = 1700 + [10^6/(F \times 10^6)^{1.39}] \tag{13}$$

Although this correlation was developed for flow over a smooth flat plate, it agrees reasonably well with the present results for flow over a hump at incipient separation (Fig. 9).

A possible extension of the present work is to correlate the minimum height of the hump which causes transition at the end of the hump with parameters such as the length of the hump, the freestream

Reynolds number and the freestream Mach number. At the end of the hump, the value of x is $(1 + \lambda/2)$. For specific values of λ, Re, and M_∞, the transition Reynolds number at the end of the hump is

$$Re_x = xRe = \left(1 + \frac{\lambda}{2}\right) Re \tag{14}$$

Using Eq. (14) in Eq. (12) and solving for F we obtain

$$F \times 10^6 = \left[\frac{254 \times 10^6}{(1 + 0.5\lambda)Re - 431800}\right]^{0.719} \tag{15}$$

The frequency F given by Eq. (15) is the frequency predicted to cause transition at the end of the hump. It is possible to consider various combinations of λ and Re and compute F from Eq. (15) and then search for the minimum height h which results in transition at the end of the hump for a given M_∞. It is then possible to analytically correlate the critical height h as a function of λ, Re, and M_∞. It is also possible to analytically correlate the roughness height that just causes incipient separation with λ, Re, and M_∞. By having the two described correlations available, it would then become very convenient to evaluate the validity of taking the separation location as the transition location in the large parameter space.

IV. Conclusions

The relationship between the locations of transition and separation in subsonic flow over a roughness element is studied. This study evaluates the customary assumption that these two locations are the same. This assumption is not valid at low unit Reynolds numbers for short roughness elements and at high (subsonic) speeds. In addition, at high unit Reynolds numbers and locations far downstream of the roughness element, the assumption is not valid because transition occurs before it reaches the roughness elements. However, the assumption works fairly well in the intermediate range.

Acknowledgment

This research is supported by the Theoretical Flow Physics Branch, Fluid Mechanics Division, NASA Langley Research Center, Hampton, Virginia, under Contract NAS1-19299.

References

[1]Fage, A., "The Smallest Size of Spanwise Surface Corrugation Which Affect Boundary Layer Transition on an Airfoil," British Aeronautical Research Council, Rept. and Memoranda 2120, 1943.

[2]Holmes, B. J., Obara, C. J., Martin, G. L., and Domack, C. S., "Manufacturing Tolerances," *Laminar Flow Aircraft Certification*, NASA CP-2413, 1986, pp. 171–183.

[3]Nayfeh, A. H., Ragab, S. A., and Al-Maaitah, A. A., "Effect of Bulges on the Stability of Boundary Layers," *Physics of Fluids A*, Vol. 31, No. 4, 1988, pp. 796–806.

[4]Ragab, S. A., Nayfeh, A. H., and Krishna, R. C., "Stability of Compressible Boundary Layers over a Smooth Backward- and Forward-Facing Step," AIAA Paper 90-1449, 1990.

[5]Masad, J. A., and Iyer, V., "Transition Prediction and Control in Subsonic Flow Over a Hump," *Physics of Fluids*, Vol. 6, No. 1, 1994, pp. 313–327; also NASA CR-4543, Sept. 1993.

[6]Cebeci, T., and Egan, D. A., "Prediction of Transition Due to Isolated Roughness," *AIAA Journal*, Vol. 27, 1989, pp. 870–875.

[7]Masad, J. A., and Nayfeh, A. H., "Stability of Separating Boundary Layers," *Proceedings of the Fourth International Conference of Fluid Mechanics* (Alexandria, Egypt), Vol. 1, 1992, pp. 261–278.

[8]Fage, A., and Preston, J. H., "On Transition from Laminar to Turbulent Flow in the Boundary Layer," *Proceedings of the Royal Society of London*, Vol. 1 178, 1941, pp. 201–227.

[9]Dryden, H. L., "Review of Published Data on the Effect of Roughness on Transition from Laminar to Turbulent Flow," *Journal of the Aeronautical Sciences*, July 1953, pp. 477–482.

[10]Nayfeh, A. H., "Influence of Two-Dimensional Imperfections on Laminar Flow," Society of Automotive Engineers, SAE Paper 92-1990, 1992.

[11]Davis, R. T., "A Procedure for Solving the Compressible Interacting Boundary Layer Equations for Subsonic and Supersonic Flows," AIAA Paper 84-1614, 1984.

[12]Smith, F. T., and Merkin, J. H., "Triple-Deck Solutions for Subsonic Flow Past Humps, Steps, Concave or Convex Corners and Wedge Trailing Edges," *Journal of Computational Physics*, Vol. 10, 1982, p. 7.

[13]Smith, F. T., Brighton, P. W. M., Jackson, P. S., and Hunt, J. C. R., "On Boundary Layer Flow Past Two-Dimensional Obstacles," *Journal of Fluid Mechanics*, Vol. 113, pp. 123–152.

[14]Gruber, K., Bestek, H., and Fasel, H., "Interaction Between a Tollmien–Schlichting Wave and a Laminar Separation Bubble," AIAA Paper 87-1256, 1987.

[15]Van Dam, C. P., and Elli, S., "Simulation of Nonlinear Tollmien–Schlichting Wave Growth Through a Laminar Separation Bubble," *Instability, Transition, and Turbulence*, edited by M. Y. Hussaini, A. Kumar, and C. L. Streett, Springer–Verlag, 1992, pp. 311–321.

[16]Pereyra, V., "PASVA3: An Adaptive Finite-Difference Fortran Program for First Order Nonlinear, Ordinary Boundary Problems," *Lecture Notes in Computer Science*, Vol. 76, 1976, pp. 67–88.

[17]Mack, L. M., "Boundary Layer Stability Theory," Jet Propulsion Lab., Document 900-277, Rev. A, Pasadena, CA, 1969.

[18]Goldstein, M. E., and Hultgren, L. S., "Boundary-Layer Receptivity to Long-Wave Free-stream Disturbances," *Annual Review of Fluid Mechanics*, Vol. 21, 1989, pp. 137–166.

[19]Braslow, A. L., and Maddalon, D. V., "Flight Tests of Three-Dimensional Surface Roughness in the High Crossflow Region of a Swept Wing with Laminar-Flow Control," NASA TM-109035, Oct. 1993.

[20]Von Doenhoff, A. E., and Braslow, A. L., "The Effect of Distributed Surface Roughness on Laminar Flow," *Boundary-Layer and Flow Control—Its Principles and Applications*, Vol. 2, Pergamon Press, 1961.

[21]Braslow, A. L., Hicks, R. M., and Harris, R. V., "Use of Grit-Type Boundary-Layer-Transition Trips on Wind-Tunnel Models," NASA TN D-3579, 1966.

[22]Masad, J. A., and Nayfeh, A. H., "Effect of a Bulge on the Subharmonic Instability of Subsonic Boundary Layers," *AIAA Journal*, Vol. 30, No. 7, 1992, pp. 1731–1737.

[23]Larson, H. K., and Keating, S. J., "Transition Reynolds Numbers of Separated Flows at Supersonic Speeds," NASA Tech. Note TN D-349, 1960.

[24]Coles, D., "Measurements of Turbulent Friction on a Smooth Flat Plate in Supersonic Flow," *Journal of the Aeronautical Sciences*, Vol. 21, No. 7, 1954, pp. 433–448.

[25]Carmichael, B. H., "Surface Waviness Criteria for Swept and Unswept Laminar Suction Wings," Northrop Aircraft Rept. NOR-59-438 (BLC-123), 1957.

[26]Morkovin, M. V., "Bypass-Transition Research: Issues and Philosophy," *Instabilities and Turbulence in Engineering Flows*, edited by D. E. Ashpis, T. B. Gatski, and R. Hirsh, Kluwer Academic, 1993, pp. 3–30.

[27]Hansman, R. J., "Microphysical Factors Which Influence Ice Accretion," *Proceedings of the First Bombardier International Workshop on Aircraft Icing and Boundary-Layer Stability and Transition*, edited by I. Paraschivoiu, ISBN 2-553-00422-2, 1993, pp. 86–103.

[28]Masad, J. A., and Malik, M. R., "Transition Correlation in Subsonic Flow over a Flat Plate," *AIAA Journal*, Vol. 31, No. 10, 1993, pp. 1953–1955.

[29]Masad, J. A., and Malik, M. R., "Comparison of Linear Stability Results with Flight Transition Data," *AIAA Journal*, Vol. 33, No. 1, pp. 161–163.